

UC San Diego

UC San Diego Previously Published Works

Title

Different polarisome components play distinct roles in Slr2p-regulated cortical ER inheritance in *Saccharomyces cerevisiae*.

Permalink

<https://escholarship.org/uc/item/4134d06s>

Journal

Cell regulation, 24(19)

Authors

Li, Xia

Ferro-Novick, Susan

Novick, Peter

Publication Date

2013-10-01

DOI

10.1091/mbc.E13-05-0268

Peer reviewed

Different polarisome components play distinct roles in Slt2p-regulated cortical ER inheritance in *Saccharomyces cerevisiae*

Xia Li^a, Susan Ferro-Novick^{a,b}, and Peter Novick^a

^aDepartment of Cellular and Molecular Medicine and ^bHoward Hughes Medical Institute, University of California, San Diego, La Jolla, CA 92093-0644

ABSTRACT Ptc1p, a type 2C protein phosphatase, is required for a late step in cortical endoplasmic reticulum (cER) inheritance in *Saccharomyces cerevisiae*. In *ptc1Δ* cells, ER tubules migrate from the mother cell and contact the bud tip, yet fail to spread around the bud cortex. This defect results from the failure to inactivate a bud tip-associated pool of the cell wall integrity mitogen-activated protein kinase, Slt2p. Here we report that the polarisome complex affects cER inheritance through its effects on Slt2p, with different components playing distinct roles: Spa2p and Pea2p are required for Slt2p retention at the bud tip, whereas Bni1p, Bud6p, and Sph1p affect the level of Slt2p activation. Depolymerization of actin relieves the *ptc1Δ* cER inheritance defect, suggesting that in this mutant the ER becomes trapped on the cytoskeleton. Loss of Sec3p also blocks ER inheritance, and, as in *ptc1Δ* cells, this block is accompanied by activation of Slt2p and is reversed by depolymerization of actin. Our results point to a common mechanism for the regulation of ER inheritance in which Slt2p activity at the bud tip controls the association of the ER with the actin-based cytoskeleton.

Monitoring Editor
Akihiko Nakano
RIKEN

Received: May 21, 2013

Revised: Jul 25, 2013

Accepted: Jul 26, 2013

INTRODUCTION

In eukaryotic cells, the endoplasmic reticulum (ER) forms a contiguous structure of tubules and sheets, all interconnected to form an extended polygonal network (Voeltz *et al.*, 2002; Du *et al.*, 2004). This network has connections to the outer membrane of the nuclear envelope and spreads throughout the cell, all the way to the cortex, where it is tethered to the inner surface of the plasma membrane. As an essential, single-copy number organelle that cannot be generated *de novo*, the ER must be actively segregated into daughter cells during cell division. The process of ER inheritance has been most extensively analyzed in the yeast *Saccharomyces cerevisiae*. The ER in yeast forms a polygonal network of sheets and tubules that lies

just beneath the plasma membrane (cortical ER [cER]), with several tubular connections through the cytoplasm to the nuclear envelope. Soon after bud emergence a new ER tubule emerges from the nuclear envelope. This segregation tubule becomes aligned along the mother–bud axis and actively extends into the daughter cell. It forms a stable contact at the tip of the bud but then quickly spreads along the cortex of the bud (Fehrenbacher *et al.*, 2002; Estrada *et al.*, 2003). Once the bud has grown to about one-third the diameter of the mother cell, the ER in the daughter cell is present predominantly in the form of a cortical network, very similar in morphology to that of the mother cell (Voeltz *et al.*, 2002; Du *et al.*, 2004).

Genetic analysis in yeast has identified a number of components of the ER inheritance machinery and defined three stages in the inheritance pathway. In strains lacking the nonessential type V myosin, Myo4p, most cells fail to form an ER segregation tubule from the nuclear envelope at the start of the cell cycle, and, when a tubule is observed, it fails to align along the mother–bud axis or extend into the daughter cell (Estrada *et al.*, 2003). Mutations in several of the exocyst genes, including *sec3Δ*, block ER inheritance at a later stage (Wiederkehr *et al.*, 2003; Reinke *et al.*, 2004). In these mutants, a tubule forms from the nuclear envelope and extends into the daughter cell but fails to form a stable attachment to the bud tip and often recedes back into the mother cell. A somewhat different phenotype

This article was published online ahead of print in MBoC in Press (<http://www.molbiolcell.org/cgi/doi/10.1091/mbc.E13-05-0268>) on August 7, 2013.

Address correspondence to: Peter Novick (pnovick@ucsd.edu).

Abbreviations used: cER, cortical endoplasmic reticulum; CWI, cell wall integrity; DIC, differential interference contrast; ER, endoplasmic reticulum; LAT-A, latrunculin A; MAPK, mitogen-activated protein kinase; Pgk1, phosphoglycerate kinase 1; SEM, standard error of the mean.

© 2013 Li *et al.* This article is distributed by The American Society for Cell Biology under license from the author(s). Two months after publication it is available to the public under an Attribution–Noncommercial–Share Alike 3.0 Unported Creative Commons License (<http://creativecommons.org/licenses/by-nc-sa/3.0>).

"ASCB®," "The American Society for Cell Biology®," and "Molecular Biology of the Cell®" are registered trademarks of The American Society of Cell Biology.

is seen in mutants lacking the serine/threonine phosphatase, Ptc1p (Du *et al.*, 2006). In *ptc1Δ* cells an ER tubule extends into the daughter cell and becomes stably attached to the bud tip, yet fails to spread along the cortex of the bud. Ptc1p controls ER inheritance by downregulating the cell wall integrity (CWI) mitogen-activated protein kinase (MAPK) pathway: loss of Ptc1p results in increased activation of Slt2p, the final kinase of the CWI MAPK cascade, and deletion of *SLT2* suppresses the ER inheritance defect of *ptc1Δ* cells (Du *et al.*, 2006). Slt2p normally undergoes cell cycle-dependent activation (Zarzov *et al.*, 1996), with the time of peak activation correlating with the time at which the initial ER tubule becomes anchored to the bud tip (Li *et al.*, 2010). The failure to inactivate Slt2p by Ptc1p-dependent dephosphorylation arrests ER inheritance at this stage. Although most Slt2p is present in the nucleus, a pool is concentrated at the tip of small buds and the neck of large-budded cells. Localization of Slt2p to the bud tip or neck requires the function of Spa2p, a component of the polarisome complex (van Drogen and Peter, 2002). Either loss of Spa2p function or mutation of a sequence within Slt2p that is needed for its bud tip localization results in suppression of the *ptc1Δ* ER inheritance defect (Li *et al.*, 2010). These findings indicate that it is the activation of a pool of Slt2p at the bud tip that serves to block the progression of ER from the bud tip to the bud cortex in *ptc1Δ* cells.

ER inheritance is also blocked in response to ER stress, such as during growth in the presence of the reducing agent dithiothreitol or the glycosylation inhibitor tunicamycin, and this response similarly requires the activation of Slt2p (Babour *et al.*, 2010). The inhibition of ER inheritance in response to stress serves to delay the segregation of nonfunctional ER into the daughter cell until the misfolded proteins accumulated within this organelle can be refolded or degraded. Thus some of the same signaling components used to control the normal cell cycle-dependent timing of ER inheritance are also used to delay inheritance in response to stress.

Ptc1p has also been implicated in the inheritance of mitochondria (Roeder *et al.*, 1998), vacuoles (Du *et al.*, 2006), and peroxisomes (Jin *et al.*, 2009). In the case of mitochondrial inheritance, as in ER inheritance, Ptc1p is needed to down-regulate Slt2p, as loss of Slt2p function suppresses the mitochondrial inheritance defect of *ptc1Δ* cells (Li *et al.*, 2010). Of interest, loss of Spa2p does not suppress the *ptc1Δ* mitochondrial inheritance defect, suggesting that it is not the bud tip-associated pool of Slt2p that controls the inheritance of this organelle (Li *et al.*, 2010).

The polarisome comprises a number of different components that associate with each other at sites of polarized cell growth, including Spa2p, Sph1p, Bni1p, Bud6p, Pea2p, Msb3p, and Msb4p. Spa2p serves as a scaffold for the other components (Sheu *et al.*, 1998), and Sph1p is a Spa2p homologue (Roemer *et al.*, 1998). The formin protein, Bni1p, catalyzes the assembly of filamentous actin cables, and its activity is promoted by Bud6p, an actin monomer-binding protein (Moseley *et al.*, 2004). The function of Pea2p is not well defined. Msb3p and Msb4p are redundant proteins that serve as GTPase-activating proteins for the rab protein, Sec4p, although they have an additional function in the regulation of the polarity establishment GTPase, Cdc42p (Tcheperegine *et al.*, 2005). Here we systematically explore the role of each of these components in the Slt2p-dependent regulation of ER inheritance.

RESULTS

Polarisome components are involved in Ptc1p-regulated cER inheritance

We previously showed that, in *ptc1Δ* mutant cells, it is the failure to inactivate the MAPK Slt2p that underlies the observed delay in the

propagation of ER segregation tubules from their docking site at the bud tip to the cortex of the growing bud (Du *et al.*, 2006). The pool of Slt2p that controls this process requires a component of the polarisome complex, Spa2p, for its retention at the bud tip (Li *et al.*, 2010). In yeast the polarisome complex has seven identified components: Bni1p, Spa2p, Pea2p, Bud6p, Sph1p, Msb3p, and Mbs4p. They are all localized to the tip of small buds and the neck of large-budded cells. We systematically examined polarisome deletions to determine whether they display genetic interactions with *ptc1Δ*. As shown in Supplemental Figure S1, deletion of each individual polarisome component gene had no effect on cell growth in a wild-type (wt) background but displayed varying synthetic growth phenotypes in a *ptc1Δ* background. The *bni1Δ ptc1Δ* and *bud6Δ ptc1Δ* double mutants grew significantly more slowly than the *ptc1Δ* single mutant, whereas the *sph1Δ ptc1Δ* strain grew faster than the *ptc1Δ* strain. The other double mutants—*msb3Δ ptc1Δ*, *msb4Δ ptc1Δ*, *pea2Δ ptc1Δ*, and *spa2Δ ptc1Δ*—displayed no significant change in growth relative to the *ptc1Δ* single mutant. Because Msb3p and Msb4p are functionally redundant proteins, we also constructed a *msb3Δ msb4Δ* double-deletion strain, which grows somewhat more slowly than wt, and found that these mutations, together, were synthetically lethal in combination with *ptc1Δ*. The varying synthetic interactions suggest that different polarisome components might play distinct roles in Ptc1p-regulated cellular processes.

We next determined whether polarisome mutations, alone or in combination with *ptc1Δ*, have any effects on ER inheritance. In wt cells, ER tubules move into newly forming buds along the mother-bud axis but then rapidly disperse to form an evenly distributed cortical network in small buds. Therefore, at any one time, only a minor fraction of small-budded cells display ER tubules along the mother-bud axis, whereas most buds (~80%) exhibit cortical ER. In *ptc1Δ* cells, >80% of small buds contain only cytoplasmic ER tubules oriented along the mother-bud axis, with no detectable cortical ER in the bud (Du *et al.*, 2006). As we previously showed, deletion of *SPA2* significantly suppresses the cortical ER inheritance defect of *ptc1Δ* cells (Li *et al.*, 2010). We found that most of the other polarisome mutations—*bud6Δ*, *bni1Δ*, *pea2Δ*, and *sph1Δ*—also significantly suppressed the cortical ER inheritance defect of *ptc1Δ* cells. As shown in Figure 1 and Supplemental Figure S2, in *bud6Δ ptc1Δ*, *bni1Δ ptc1Δ*, *pea2Δ ptc1Δ*, *sph1Δ ptc1Δ*, and *spa2Δ ptc1Δ* double-mutant cells, only ~10–30% of small buds exhibited ER tubules along the mother-bud axis, and ~70–90% of small buds possessed a well-distributed cortical ER network. Two polarisome component mutations, *msb3Δ* and *msb4Δ*, had no suppression activity, possibly because these two gene products are redundant. Owing to the inviability of the *msb3Δ msb4Δ ptc1Δ* triple mutant, we were unable to assess the suppression activity of simultaneously deleting both *MSB* genes.

Polarisome components play distinct roles in Slt2p function, affecting either its localization or its activity

Activation of Slt2p at the bud tip leads to a delay in the distribution of ER tubules to the bud cortex in *ptc1Δ* mutant cells (Li *et al.*, 2010). Polarisome mutations could suppress the ER inheritance defect in *ptc1Δ* cells either by regulating Slt2p localization at the bud tip, as shown for Spa2p (Li *et al.*, 2010), or controlling the level of Slt2p activation. If a polarisome mutation disrupts the localization of Slt2p to the bud tip, even though Slt2p is still activated in *ptc1Δ* cells, it would not be able to phosphorylate the relevant downstream substrate at the bud tip to block cER spreading. Alternatively, if the polarisome mutation decreases the level of Slt2p activation without affecting localization, it would antagonize Slt2p function and thereby restore normal cER inheritance.

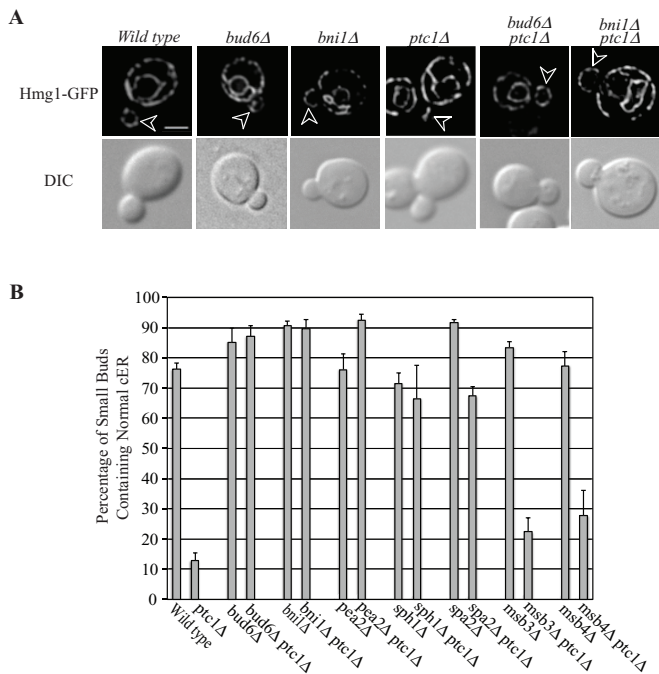


FIGURE 1: Deletion of individual polarisome component genes (except *msb3* and *msb4*) significantly suppresses the cER inheritance defects in *ptc1Δ* mutant cells. (A) Representative GFP fluorescence of ER marker Hmg1p and differential interference contrast (DIC) images of wt, *bud6Δ*, *bni1Δ*, *ptc1Δ*, *bud6Δptc1Δ*, and *bni1Δptc1Δ* cells grown to early log phase in SC medium at 25°C (*sph1Δ*, *sph1Δptc1Δ*, *pea2Δ*, *pea2Δptc1Δ*, *spa2Δ*, *spa2Δptc1Δ*, *msb3Δ*, *msb3Δptc1Δ*, *msb4Δ*, and *msb4Δptc1Δ* images are shown in Supplemental Figure S2). Arrowheads point to small buds. Bar, 5 μm. (B) The percentage of small buds that contained normal cortical ER in indicated strains was quantified. Error bars, SEM from three independent experiments.

To address these two possible mechanisms, we assessed Slt2p localization and activation in the various polarisome deletion mutants. We used a plasmid expressing an Slt2p–green fluorescent protein (GFP) fusion from the endogenous *SLT2* promoter. Slt2p–GFP is predominantly nuclear at all stages of the cell cycle, yet also localizes to the tip of small buds and to the bud neck late in mitosis (large buds). Approximately 70% of small buds exhibit a concentration of Slt2p–GFP at the bud tip in a wt strain. Deletion of the polarisome gene *PEA2* reduced Slt2p–GFP localization at bud tips (Figure 2, A and B), as shown for the deletion of *SPA2* (van Drogen and Peter, 2002). In contrast, the deletion of other polarisome component genes did not significantly affect Slt2p–GFP localization at bud tips (Figure 2 and Supplemental Figure S3).

Slt2p is the final kinase of the CWI MAPK cascade (Levin, 2005). It is activated by a series of upstream kinases: MEKK1 (Bck1p) and the MEKs (Mkk1p and Mkk2p). Mkk1p and Mkk2p are two redundant kinases that, like Slt2p, are localized in part at sites of polarized growth. We explored the possibility that one or more polarisome components are required for localization of Mkk1p or Mkk2p at bud tips. A previous study indicated a role for Spa2p in Mkk1p localization (van Drogen and Peter, 2002). We used a GFP fusion protein, Mkk1p–GFP, expressed from the *ADH1* promoter and followed its localization in wt and polarisome mutant cells. Mkk1p–GFP is localized at the tips of small buds and at the mother–bud neck in large-budded cells. The deletion of polarisome gene *BUD6*, *BNI1*, or *SPH1* did not affect Mkk1p–GFP localization at bud tips or bud necks

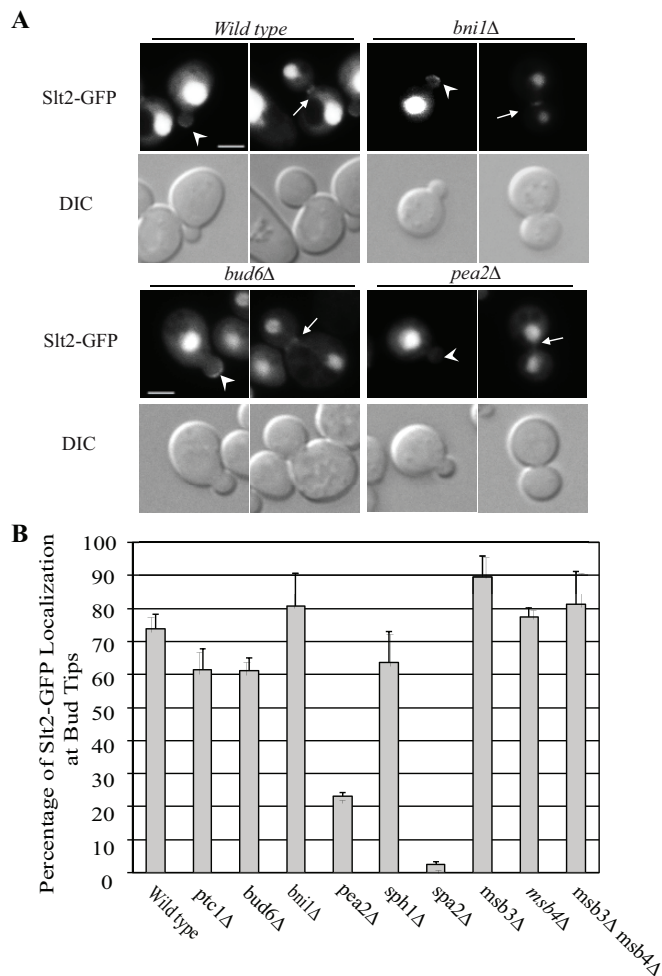


FIGURE 2: Deletion of *PEA2* or *SPA2* affects Slt2–GFP localization at bud tip or bud neck, whereas the deletion of other polarisome component genes does not. (A) Slt2–GFP fluorescence and DIC images of representative cells grown to early log phase in SC medium at 25°C. The strains shown are wt, *ptc1Δ*, *bud6Δ*, *bni1Δ*, *pea2Δ*, *sph1Δ*, *spa2Δ*, *msb3Δ*, *msb4Δ*, or *msb3Δmsb4Δ* double mutant containing a plasmid expressing an Slt2–GFP fusion from the endogenous promoter (*ptc1Δ*, *sph1Δ*, *spa2Δ*, *msb3Δ*, *msb4Δ*, and *msb3Δmsb4Δ* images are shown in Supplemental Figure S3). Arrowheads and arrows point to the bud tip in small buds and bud neck in large buds, respectively. Bars, 5 μm. (B) The Slt2–GFP localization in small buds from the strains examined was quantified. Error bars in the bar graph are SEM from three independent experiments.

(Supplemental Figure S4), whereas *pea2Δ* decreased Mkk1p localization, as shown for *spa2Δ* (van Drogen and Peter, 2002).

We next determined whether the activation of Slt2p by phosphorylation is affected by loss of any of the polarisome components. Whole-cell lysates from the indicated strains were blotted using an antibody that specifically recognizes only the active, phosphorylated form of Slt2p or an antibody that recognizes the total pool of Slt2p. The results are shown separately for convenience (Figure 3A), with the cytoplasmic protein Pgk1p used as a loading control. The total pool of Slt2p exhibited only modest differences between the various strains (Figure 3A). In wt cells, Slt2p undergoes both phosphorylation and dephosphorylation, and hence at steady state, a low level of active Slt2p was detected by Western blot analysis. In *ptc1Δ* cells, dephosphorylation of Slt2p is blocked, leading to a large increase of

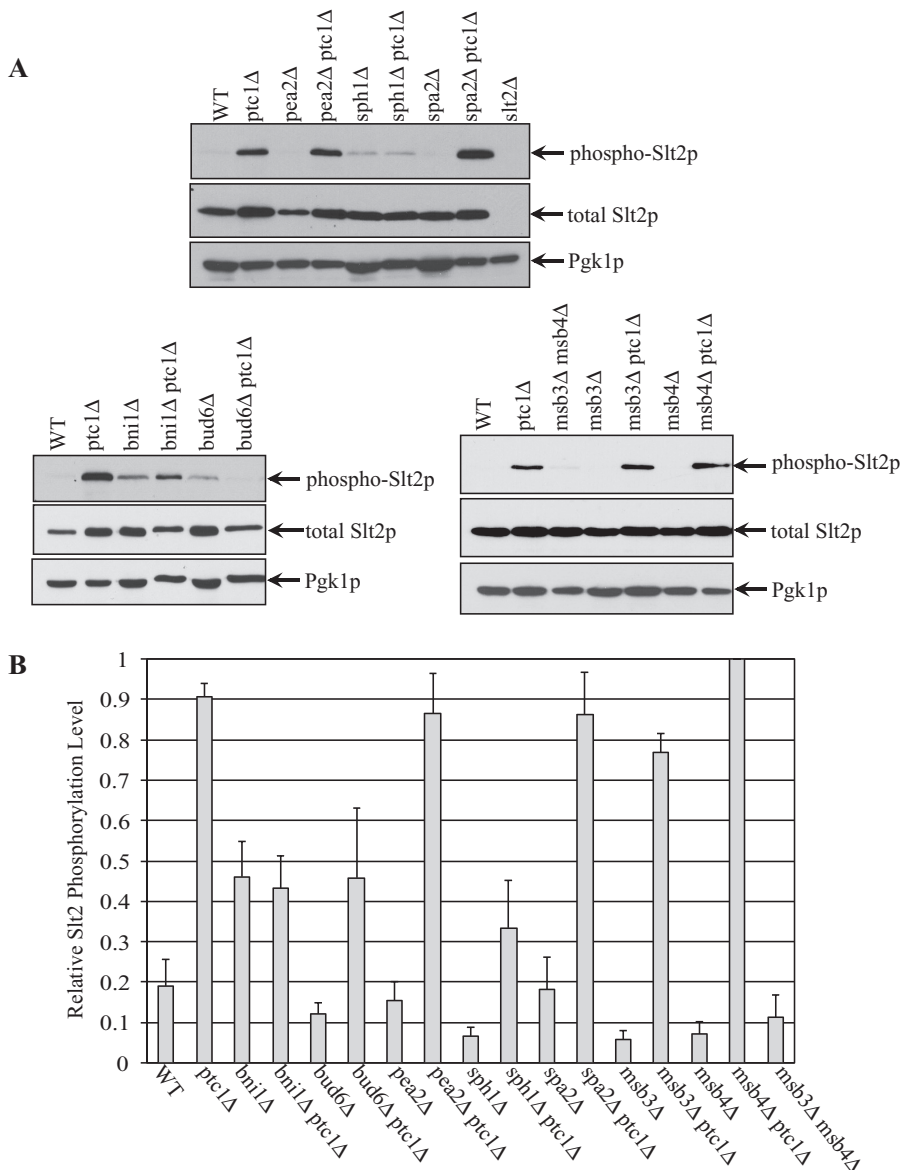


FIGURE 3: Loss of *Bni1p*, *Bud6p* or *Sph1p* decreases the level of activated Slt2p in *ptc1Δ* mutant cells. (A) Yeast lysates were extracted separately from strains wt, *ptc1Δ*, *pea2Δ*, *pea2Δptc1Δ*, *sph1Δ*, *sph1Δptc1Δ*, *spa2Δ*, and *spa2Δptc1Δ* (top), *bni1Δ*, *bni1Δ ptc1Δ*, *bud6Δ*, *bud6Δ ptc1Δ* (bottom, left), or *msb3Δmsb4Δ*, *msb3Δ*, *msb3Δptc1Δ*, *msb4Δ*, and *msb4Δptc1Δ* (bottom, right). Slt2p activation was measured as the intensity of dually phosphorylated Slt2p on Western blots, and the total Slt2p protein level in the same sample was measured using anti-Slt2p blots. Pgk1p was used as a loading control. (B) The relative phosphorylation level of Slt2p from the strains examined was quantified. The density of the phospho-Slt2p band was divided by the density of Pgk1p, and the normalized phospho-Slt2p value of each strain is shown in the bar graph. Error bars, SEM from four independent experiments.

the active, phosphorylated pool. In polarisome gene deletion mutants *bni1Δ*, *bud6Δ*, *pea2Δ*, *sph1Δ*, and *spa2Δ*, we detected very low levels of active Slt2p. The *bni1Δptc1Δ*, *bud6Δptc1Δ*, and *sph1Δptc1Δ* double mutants had significantly decreased pools of active Slt2p relative to the *ptc1Δ* single mutant (Figure 3). This suggests that these polarisome components play a role in Slt2p activation, which in turn would affect cER inheritance. In contrast, the *pea2Δ ptc1Δ* and *spa2Δ ptc1Δ* double mutants did not significantly reduce the level of Slt2p activation relative to the *ptc1Δ* single mutant.

The deletion of *MSB3* or *MSB4* in wt or *ptc1Δ* cells had no effect on either Slt2p-GFP localization (Supplemental Figure S3) or the

level of Slt2p phosphorylation (Figure 3). This is consistent with their failure to suppress the cER inheritance defect of *ptc1Δ* cells. Slt2-GFP localization also appeared to be unaffected in an *msb3Δ msb4Δ* double-mutant strain (Supplemental Figure S3). The *msb3Δ msb4Δ* double mutant displayed only a low level of phospho-Slt2p; due to the inviability of *msb3Δ msb4Δ ptc1Δ* triple mutants; however, we were unable to test the effects of the combined loss of *Msb3* and *Msb4* on Slt2p activation. Taken together, all components of the polarisome, with the possible exception of *Msb3p* and *Msb4p*, affect the function of Slt2p in the regulation of cortical ER inheritance. *Pea2p* and *Spa2p* are needed to recruit Slt2p to bud tips, and *Bni1p*, *Bud6p*, and *Sph1p* affect the level of Slt2p activation.

Depolymerization of the actin cytoskeleton bypasses *Ptc1p* and *Sec3p* function in ER inheritance

Ptc1p promotes vacuolar inheritance by facilitating the interaction of the type V myosin, *Myo2p*, with *Vac17p*, a receptor on the surface of the vacuole, and it has been suggested that *Ptc1p* might control the inheritance of other organelles by related mechanisms (Jin *et al.*, 2009). In *ptc1Δ* mutant cells, ER tubules migrate into the bud but fail to spread along the bud cortex (Du *et al.*, 2006). Because *Myo4p* drives the vectorial movement of ER segregation tubules into the bud (Estrada *et al.*, 2003), it appears that the connection between the ER and this motor must be functional in the absence of *Ptc1p*. Nonetheless, one possible explanation for the ER inheritance phenotype of *ptc1Δ* cells is that the connection between *Myo4p* and the ER persists even after the tubules have been delivered to the bud, such that they are not free to propagate along the cortex but instead remain trapped on actin cables. To explore this possibility, we treated *ptc1Δ* cells with the actin depolymerization reagent latrunculin A. Remarkably, after only 10 min of latrunculin A treatment the cytoplasmic ER tubules in the buds of *ptc1Δ* cells were replaced with normal cortical ER (Figure 4). Time-lapse microscopy suggests that the ER tubule present in the bud of *ptc1Δ* cells spreads along the bud cortex in response to the addition of latrunculin A (Supplemental Figure S5). Therefore we propose that in *ptc1Δ* cells, the ER fails to spread to the cortex of the bud because it is bound to the actin cytoskeleton. This result also implies that the propagation of ER along the cortex of the bud is not an actin-dependent process.

In *sec3Δ* cells, as in *ptc1Δ* cells, ER tubules extend into the bud but fail to propagate along the cortex (Wiederkehr *et al.*, 2003). Addition of latrunculin A to *sec3Δ* cells reversed this ER phenotype (Figure 4). The ER tubules extending into the bud, typical of *sec3Δ*

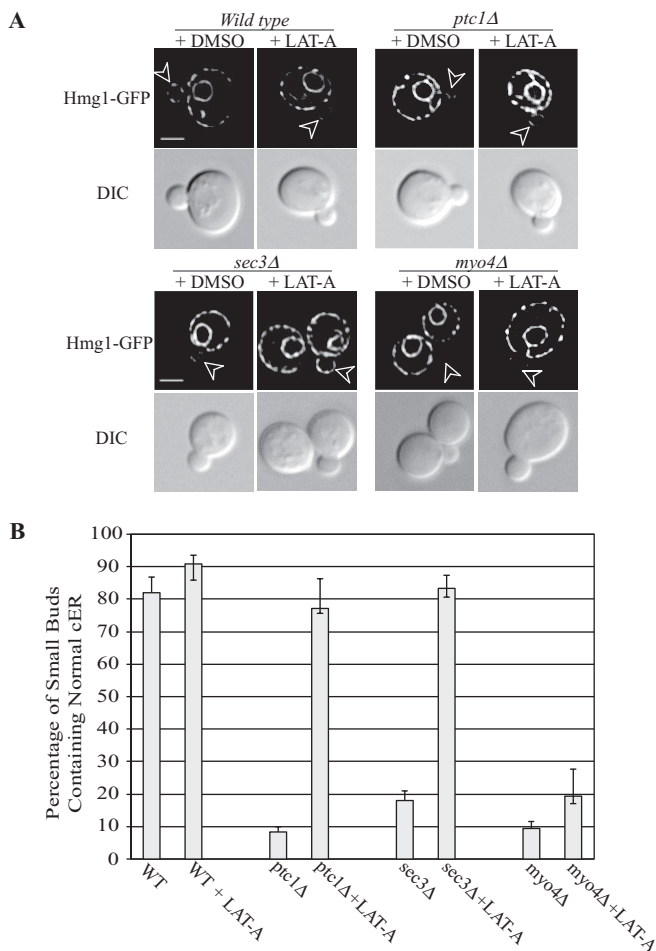


FIGURE 4: The effects of latrunculin A (Lat-A) treatment on cER inheritance in wild-type or mutant cells (*ptc1Δ*, *sec3Δ* or *myo4Δ*). Wild-type or mutant yeast cells grown to early log phase in SC medium at 25°C were incubated with control dimethyl sulfoxide or 200 μM Lat-A for 10 min. Cells were immediately fixed, washed, and then imaged with the ER marker Hmg1p-GFP. (A) Representative cell staining. Arrowheads point to small buds. (B) Percentage of cells with small buds containing normal cER staining with or without Lat-A treatment. Error bars in the bar graph represent SEM from three independent experiments.

cells, were no longer observed and were replaced by normal, cortical ER in the bud. Time-lapse microscopy suggests that the ER tubule in the bud spreads along the bud cortex in response to latrunculin A (Supplemental Figure S5). The *myo4Δ* mutant is partially defective in the formation of ER segregation tubules. In contrast to *ptc1Δ* and *sec3Δ* cells, the ER phenotype of *myo4Δ* cells was not suppressed by addition of latrunculin A (Figure 4).

sec3Δ* cells have elevated levels of phospho-Slt2p, and their ER phenotype is suppressed by loss of *bud6

The restoration of cER in small buds of both *ptc1Δ* and *sec3Δ* cells upon addition of latrunculin A suggested the possibility of a common underlying mechanism in their ER inheritance defects. We therefore measured the level of Slt2p phosphorylation in *sec3Δ* cells and found it to be elevated to a level similar to that of *ptc1Δ* cells (Figure 5, A and B, lanes 1–4). To determine whether the increased activation of Slt2p in *sec3Δ* cells was responsible for the observed ER inheritance defect, we attempted to construct a *sec3Δ slt2Δ*

double mutant; however, these mutations proved to be synthetically lethal in combination (Figure 5C). Therefore we constructed double mutants that combined *sec3Δ* with deletions of the various polarisome components, since these are required for either Slt2p localization or activation. The *pea2Δ sec3Δ* and *spa2Δ sec3Δ* double mutants were viable and grew somewhat more rapidly than the *sec3Δ* single mutant, whereas the *bni1Δ sec3Δ* double mutant was inviable. Although some of the *bud6Δ sec3Δ* double-mutant spores were inviable, others grew, albeit more slowly than the *sec3Δ* single mutant (Figure 5C).

We found that deletion of either *pea2* or *spa2* had no effect on the ER inheritance phenotype or the elevated Slt2 activation of *sec3Δ* cells, whereas loss of *bud6* largely restored normal cortical ER morphology to *sec3Δ* cells (Figure 6, A and B) and reduced the level of phospho-Slt2p (Figure 5, A, lanes 5–9, and B). Thus an interesting pattern emerged: loss of either of the two polarisome components needed for Slt2p localization had no effect on the ER inheritance phenotype of *sec3Δ* cells, whereas loss of one of the components needed for Slt2p activation did suppress the ER inheritance phenotype. One interpretation of these results is that loss of Sec3p triggers the activation of a pool of Slt2p, which in turn affects cER inheritance. This pool of Slt2p requires Bud6p for activation, yet, unlike the situation in *ptc1Δ* cells, it does not depend on Spa2p or Pea2p and therefore may act at a site other than the bud tip. This difference is consistent with the somewhat different ER inheritance phenotypes of *sec3Δ* and *ptc1Δ* cells. Because *bud6Δ* cells exhibit a modest defect in actin structure (Amberg *et al.*, 1997), it is also possible that this, rather than the loss of Slt2p activation, is the basis of the suppression of the *sec3Δ* ER phenotype.

Polarisome components are not involved in Ptc1p-regulated mitochondrial inheritance

Mitochondrial inheritance, like ER inheritance, requires Ptc1p function (Roeder *et al.*, 1998), and, as in the case of ER inheritance, the *ptc1Δ* mitochondrial inheritance phenotype is suppressed by deletion of *SLT2* (Li *et al.*, 2010). We nevertheless noted an important distinction: the mitochondrial inheritance phenotype of *ptc1Δ* is not suppressed by deletion of *SPA2*, suggesting that the relevant pool of Slt2p is not at the bud tip (Li *et al.*, 2010). We predicted that the other polarisome components would similarly not be involved in the regulation of mitochondrial inheritance. As shown in Figure 7, mitochondrial segregation structures migrate into the small buds of wt cells, whereas in *ptc1Δ* cells mitochondria remain entirely within the mother cell. Deletion of individual polarisome genes failed to suppress the mitochondrial inheritance defects in *ptc1Δ* mutant cells. The percentage of small buds containing mitochondrial segregation structures in *bud6Δptc1*, *bni1Δptc1*, *pea2Δptc1*, *sph1Δptc1*, *spa2Δptc1*, *msb3Δptc1*, and *msb4Δptc1* double-mutant cells was ~10–20%, similar to that in *ptc1Δ* cells. We also examined whether disruption of actin with latrunculin A would restore mitochondrial inheritance in *ptc1Δ* cells (Supplemental Figure S6); no restoration was seen. The difference in polarisome and actin involvement in cER inheritance versus mitochondrial inheritance again confirms the requirement for distinct pools of Slt2p in the inheritance of these two organelles. Most of the single-polarisome-gene deletions did not exhibit mitochondrial inheritance defects; however, *bud6Δ* and *bni1Δ* cells displayed partial defects, and a marginally significant inheritance defect was seen in *pea2Δ* cells (Figure 7).

DISCUSSION

We systematically explored the requirements for the components of the polarisome in Slt2p-dependent regulation of cER inheritance.

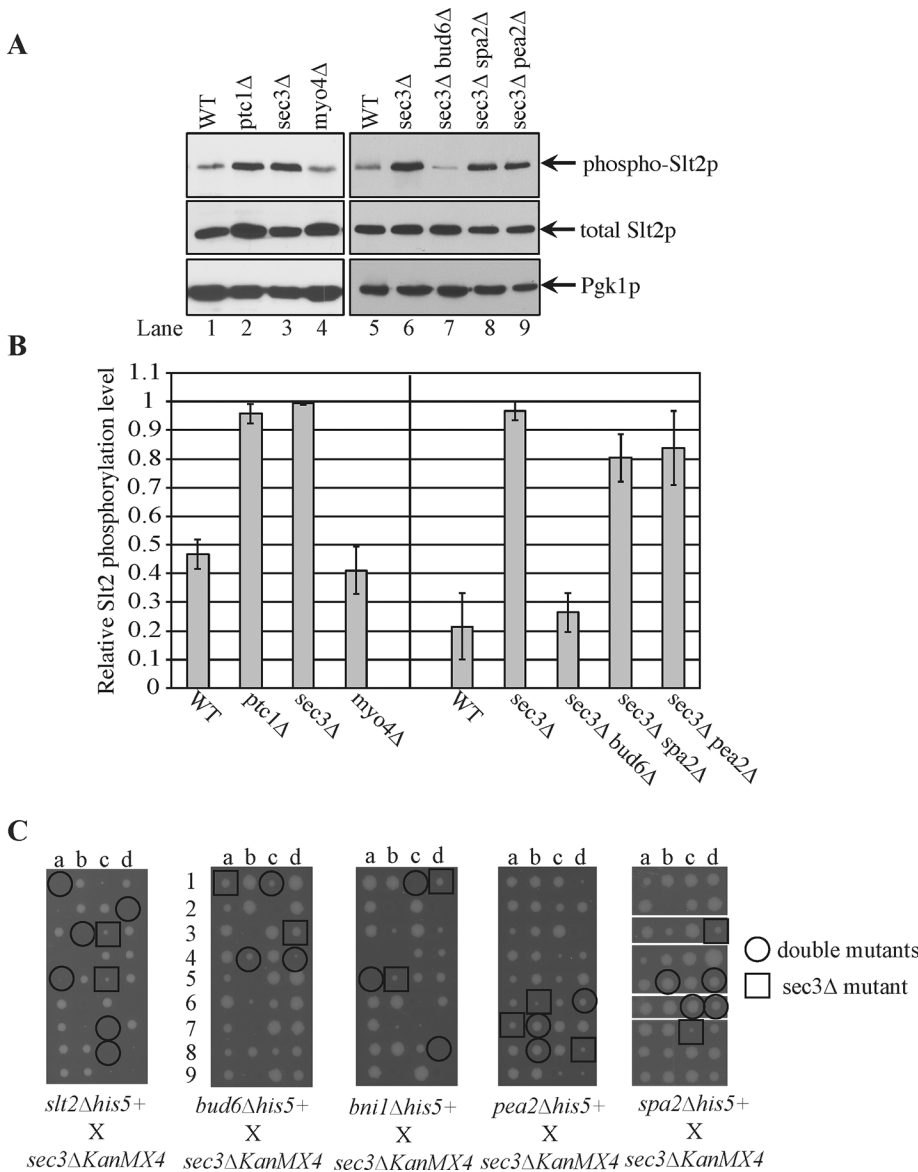


FIGURE 5: The effects of polarisome mutations on Slt2p activation level and cell growth in *sec3Δ* cells. (A) Yeast lysates were extracted separately from strains wt, *ptc1Δ*, *sec3Δ*, and *myo4Δ* (lanes 1–4) or from strains wt, *sec3Δ*, *sec3Δbud6Δ*, *sec3Δspa2Δ*, and *sec3Δpea2Δ* (lanes 5–9) and blotted using antibody that specifically recognizes dually phosphorylated Slt2p (top) or the total Slt2p (middle). Pgk1p was used as a loading control. (B) The relative activation level of Slt2p was quantified from the blots. Error bars, SEM from three independent experiments. (C) Tetrad dissection analysis with *sec3Δ*. Tetrad dissection plates from the indicated crosses are shown with representative double-deletion mutant spores circled and representative single *sec3Δ* spores squared. Replica plating to infer genotype later showed that the inviable spores were double mutants. In the cross of *sec3Δ* to *spa2Δ*, spores were dissected onto two different plates, and empty regions of the plates were deleted as indicated by the white borders.

Our results indicate that different components play different roles. *Spa2p* and *Pea2p* are needed for the localization of Slt2p and the upstream kinase, Mkk1p, to the bud tip. In the absence of these components, even though the level of Slt2p activation rises in response to the loss of the Ptc1p phosphatase, the active kinase is not concentrated at the tip of the bud. Although we do not know the substrate of Slt2p responsible for delaying cER inheritance, we can predict that it too must be present at the bud tip. This localization would be consistent with the stage at which cER inheritance is delayed in *ptc1Δ* cells; the segregation tubule extends into the bud,

anchors at the bud tip, but fails to spread along the cortex of the bud (Du *et al.*, 2006). Phosphorylation by Slt2p of a key component at the bud tip may trap the ER segregation tubule at this site, stabilizing a normally transient step in the inheritance process. Of interest, *Scs2p*, a VAP homologue needed to tether the ER to the plasma membrane, concentrates at bud tips in a *Spa2p*-dependent manner, and loss of *Scs2p* leads to a reduction in cER (Loewen *et al.*, 2007; Manford *et al.*, 2012).

Ptc1p has been proposed to regulate organelle inheritance by controlling the association of myosin motors with receptors on the surface of the affected organelles (Jin *et al.*, 2009). The restoration of cortical ER in *ptc1Δ* cells in response to the depolymerization of actin is broadly consistent with this model. Activation of Slt2p at the bud tip might stabilize the interaction between the Myo4p motor and a component on the surface of the ER (Figure 8). This would lead to the persistence of ER segregation tubules bound to actin fibers oriented along the mother–bud axis. Depolymerization of actin fibers by addition of latrunculin A would then free those ER tubules to distribute along the cortex of the bud. This is somewhat different from the proposed role of phosphorylation in vacuole inheritance. In that case, increased phosphorylation resulting from the loss of the Ptc1p phosphatase inhibits the interaction of Myo2p with the vacuole, blocking an early stage in the vacuole inheritance pathway (Jin *et al.*, 2009).

Three other components of the polarisome—*Bni1p*, *Sph1p*, and *Bud6p*—are also required for the Slt2p-dependent block in cER inheritance. In contrast to *Spa2p* and *Pea2p*, however, these components are not required for the localization of Slt2p to the bud tip. Instead, these components are needed for full activation of Slt2p in response to loss of Ptc1p function (Figure 8). Further studies will be needed to define the mechanism by which these components affect Slt2p activation. Nonetheless, our results extend the evidence for inhibition of cER inheritance by a pool of active Slt2p at the bud tip.

The remaining components of the polarisome—*Msb3p* and *Msb4p*—are functionally redundant. Therefore it is not surprising that the loss of either one alone has no effect on the *ptc1Δ* cER inheritance defect. These results are also consistent with the observation that neither of these mutations, alone, affects Slt2p localization or activation. Although we found no effect of an *msb3Δ msb4Δ* double mutant on Slt2p localization, the synthetic lethality of *ptc1Δ* in this double mutant precluded us from testing the effects of a simultaneous loss of both *MSB* genes on Slt2p activation.

The ER inheritance defect of *sec3Δ* cells, like that of *ptc1Δ* cells, is reversed by addition of latrunculin A, and the level of Slt2p activation

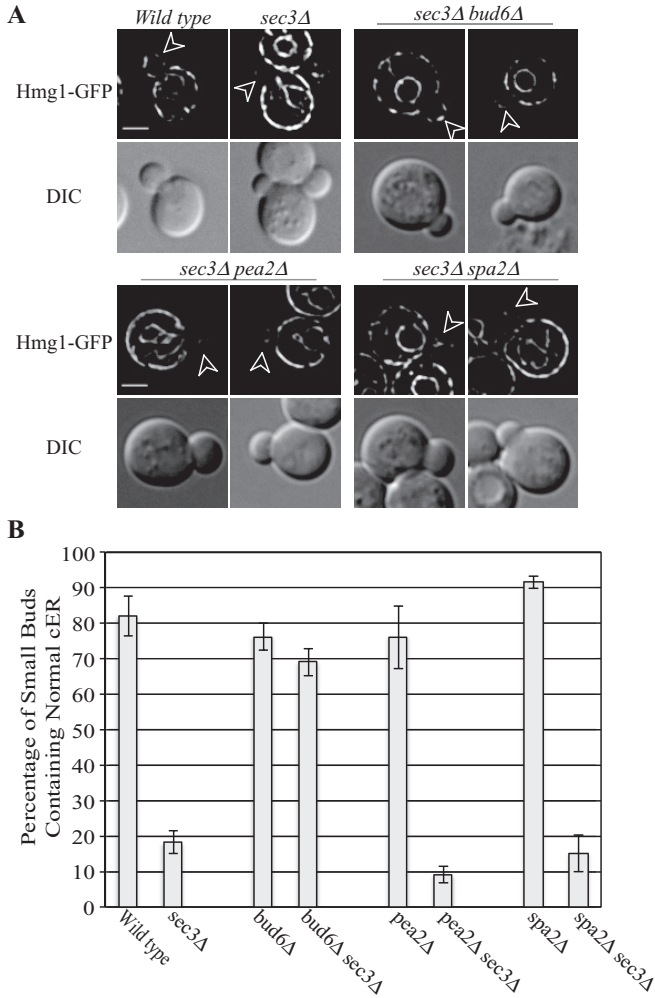


FIGURE 6: Effects of polarisome mutations on cER inheritance in *sec3Δ* cells. (A) Representative GFP fluorescence of the ER marker Hmg1-GFP and DIC images of wt, *sec3Δ*, *sec3Δbud6Δ*, *sec3Δpea2Δ*, and *sec3Δspa2Δ* cells grown to early log phase in SC medium at 25°C. Arrowheads point to small buds. Bars, 5 μm. (B) The percentage of small buds that contained normal cortical ER in indicated strains was quantified. Error bars, SEM from three independent experiments.

in *sec3Δ* cells is similar to that of *ptc1Δ* cells, suggesting a common underlying mechanism. Nonetheless, the ER defect of *sec3Δ* cells is not suppressed by loss of either Pea2p or Spa2p, although it is suppressed by loss of Bud6p, which reduces the level of Slt2p activation. Taken together, these results suggest that, in *sec3Δ* cells, Slt2p is activated by a Bud6p-dependent pathway, yet the relevant pool of Slt2p is not localized to the bud tip by Pea2p and Spa2p. This is consistent with the observation that the ER tubules that migrate into the bud in *sec3Δ* cells are not anchored at the bud tip, as they are in *ptc1Δ* cells.

Although we previously demonstrated that the mitochondrial inheritance defect of *ptc1Δ* cells is suppressed by the disruption of *SLT2* (Li *et al.*, 2010), this defect was not suppressed by the loss of any of the polarisome components. Thus the inhibition of mitochondrial inheritance in *ptc1Δ* cells relies on a pool of Slt2p that functions independently of the polarisome. The relevant pool is therefore not at the bud tip, and its activation does not require Bni1p, Sph1p, or Bud6p. These findings are consistent with the observation that in *ptc1Δ* cells, mitochondrial inheritance is blocked

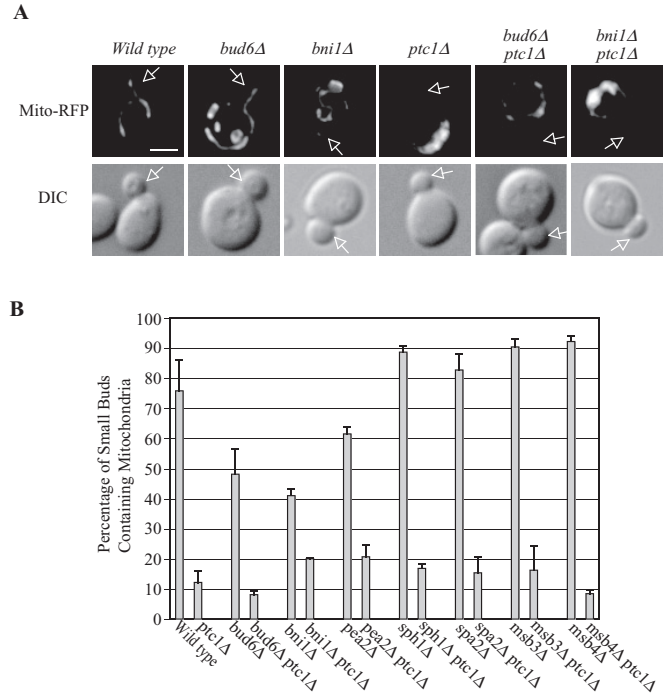


FIGURE 7: Deletion of individual polarisome component genes does not suppress the mitochondrial inheritance defect in *ptc1Δ* cells. (A) Representative fluorescence and DIC images of wt, *ptc1Δ*, *bud6Δ*, *bud6Δptc1Δ*, *bni1Δ*, *bni1Δptc1Δ*, and *sph1Δ* cells grown to early log phase in SC medium at 25°C (*sph1Δ*, *sph1Δptc1Δ*, *pea2Δ*, *pea2Δptc1Δ*, *spa2Δ*, *spa2Δptc1Δ*, *msb3Δ*, *msb3Δptc1Δ*, *msb4Δ*, and *msb4Δptc1Δ* images not shown). A plasmid expressing the F₀ATP synthase mitochondrial targeting sequence fused to RFP (Mito-RFP) was used to label mitochondria. Arrows point to small buds. Bar, 5 μm. (B) The percentage of small buds containing normal mitochondrial segregation structures in the indicated strains was quantified. Error bars, SEM from three independent experiments.

before tubules enter the daughter. This represents an earlier stage in organelle delivery than the cER inheritance defect of *ptc1Δ* cells.

The regulation of cER inheritance during the cell cycle and the comparison to mitochondrial inheritance highlight the flexibility,

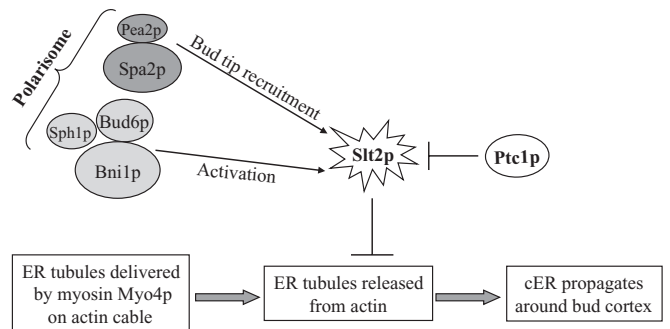


FIGURE 8: A model for the role of Slt2p and the polarisome in ER inheritance. ER tubules are delivered into the bud by the myosin Myo4p. The tubules must be released from actin structures before they can propagate around the cortex of the bud. In *ptc1Δ* cells Slt2p becomes highly activated, blocking release of ER tubules from actin. This function of Slt2p requires the polarisome components Pea2p and Spa2p for its retention at the bud tip and the components Bud6p, Bni1p, and Sph1p for its activation.

subtlety, and complexity of the signaling pathways involved. Although in both cases regulation of inheritance uses the SlT2p kinase as a key component, different pools are used in different situations. Identification of the relevant substrates of SlT2p in each situation will be critical.

MATERIALS AND METHODS

Strain construction

Table 1 lists the yeast strains used in this study. NY2959 (*MAT α* , *ptc1 Δ ::his5⁺*) and NY2965 (*MAT α* , *ptc1 Δ ::KanMX4*) were generated by replacing the *PTC1* coding sequence in BY4742 and SEY6210.1

Strain	Genotype	Source	Strain	Genotype	Source
NY1210	<i>MATα his3-200 leu2-3, 112 ura3-52</i>	Novick lab collection	NY2975	<i>MATα his3-200 leu2-3112 ura3-52 ptc1Δ::his5⁺ spa2Δ::KanMX4</i>	This study
NY1211	<i>MATα a his3-200 leu2-3, 112 ura3-52</i>	Novick lab collection	BY4742	<i>MATα MET15 his3-Δ1 lys2-Δ0 leu2-Δ0 ura3-Δ0</i>	Deletion library
NY2920	<i>MATα his3-200 leu2-3, 112 ura3-52 ptc1Δ:: his5⁺</i>	Novick lab collection	NY2959	<i>MATα MET15 his3-Δ1 lys2-Δ0 leu2-Δ0 ura3-Δ0 ptc1Δ::his5⁺</i>	This study
SFNY1683	<i>MATα his3-200 leu2-3, 112 ura3-52::(URA3, HMG1-GFP)</i>	Ferro-Novick lab collection	NY3030	<i>MATα his3-Δ1 lys2-Δ0 leu2-Δ0 ura3-Δ0 sph1Δ::KanMX4</i>	Deletion library
SFNY1684	<i>MATα his3-200 leu2-3, 112 ura3-52::(URA3, HMG1-GFP) ptc1Δ:: his5⁺</i>	Ferro-Novick lab collection	NY2960	<i>MATα his3-Δ1 lys2-Δ0 leu2-Δ0 ura3-Δ0 ptc1Δ::his5⁺ sph1Δ::KanMX4</i>	This study
SFNY1235	<i>MATα his3-200 leu2-3, 112 ura3-52 myo4Δ::his5⁺</i>	Ferro-Novick lab collection	SEY6210	<i>MATα his3-200 trp1-Δ901 lys2-801 suc2-Δ9 leu2-3, 112 ura3-52</i>	Emr lab collection
SFNY1153	<i>MATα his3-200 leu2-3, 112 ura3-52::(URA3, HMG1-GFP) sec3Δ::kanMX4</i>	Ferro-Novick lab collection	SEY6210.1	<i>MATα his3-200 trp1-Δ901 lys2-801 suc2-Δ9 leu2-3112 ura3-52</i>	Emr lab collection
SFNY1154	<i>MATα his3-200 leu2-3, 112 ura3-52::(URA3, HMG1-GFP) sec3Δ::kanMX4</i>	Ferro-Novick lab collection	NY2965	<i>MATα his3-200 trp1-Δ901 lys2-801 suc2-Δ9 leu2-3112 ura3-52 ptc1Δ::KanMX4</i>	This study
NY3020	<i>MATα his3-200 leu2-3, 112 ura3-52 slt2Δ:: his5⁺</i>	This study	NY2963	<i>MATα his3-200 trp1-Δ901 lys2-801 suc2-Δ9 leu2-3, 112 ura3-52 pea2Δ::his5⁺</i>	This study
NY3022	<i>MATα his3-200 leu2-3, 112 ura3-52 spa2Δ::his5⁺</i>	This study	NY2964	<i>MATα his3-200 trp1-Δ901 lys2-801 suc2-Δ9 leu2-3, 112 ura3-52 ptc1Δ::KanMX4 pea2Δ::his5⁺</i>	This study
NY3023	<i>MATα his3-200 leu2-3, 112 ura3-52 pea2Δ::his5⁺</i>	This study	NY2966	<i>MATα his3-200 trp1-Δ901 lys2-801 suc2-Δ9 leu2-3, 112 ura3-52 bni1Δ::his5⁺</i>	This study
NY3025	<i>MATα his3-200 leu2-3, 112 ura3-52 bni1Δ::his5⁺</i>	This study	NY2967	<i>MATα his3-200 trp1-Δ901 lys2-801 suc2-Δ9 leu2-3, 112 ura3-52 bni1Δ::his5⁺ ptc1Δ::KanMX4</i>	This study
NY3024	<i>MATα his3-200 leu2-3, 112 ura3-52 bud6Δ::his5⁺</i>	This study	NY2970	<i>MATα his3-200 trp1-Δ901 lys2-801 suc2-Δ9 leu2-3, 112 ura3-52 msb3Δ::his5⁺</i>	This study
NY3028	<i>MATα his3-200 leu2-3, 112 ura3-52::(URA3, HMG1-GFP) bud6Δ::his5 sec3Δ::kanMX4</i>	This study	NY2971	<i>MATα his3-200 trp1-Δ901 lys2-801 suc2-Δ9 leu2-3, 112 ura3-52 msb4Δ::his5⁺</i>	This study
NY3027	<i>MATα his3-200 leu2-3, 112 ura3-52::(URA3, HMG1-GFP) pea2Δ::his5 sec3Δ::kanMX4</i>	This study	NY2972	<i>MATα his3-200 trp1-Δ901 lys2-801 leu2-3, 112 ura3-52 msb3Δ::his5⁺ ptc1Δ::KanMX4</i>	This study
NY3026	<i>MATα his3-200 leu2-3, 112 ura3-52::(URA3, HMG1-GFP) spa2::his5 sec3Δ::kanMX4</i>	This study	NY2973	<i>MATα his3-200 trp1-Δ901 lys2-801 leu2-3, 112 ura3-52 msb4Δ::his5⁺ ptc1Δ::KanMX4</i>	This study
NY2968	<i>MATα his3-200 leu2-3, 112 ura3-52 bud6Δ::KanMX4</i>	This study	NY2976	<i>MATα his3-200 trp1-Δ901 lys2-801 leu2-3, 112 ura3-52 msb3Δ::his5⁺ msb4Δ::TRP1</i>	This study
NY2969	<i>MATα his3-200 leu2-3, 112 ura3-52 bud6Δ::KanMX4 ptc1Δ:: his5⁺</i>	This study			
NY2974	<i>MATα his3-200 leu2-3112 ura3-52 spa2Δ::KanMX4</i>	This study			

TABLE 1: Yeast strains used in this work.

(wild-type strains generously provided by Scott Emr, Cornell University, Ithaca, NY), respectively, with the *Schizosaccharomyces pombe* *his5⁺* gene or the KanMX4 module using the PCR-mediated gene deletion method (Longtine *et al.*, 1998). To construct individual polarisome component mutant strains *pea2Δ* (NY2963), *bni1Δ* (NY2966), *msb3Δ* (NY2970), *msb4Δ* (NY2971), *bud6Δ* (NY2968), and *spa2Δ* (NY2974) or another set of strains in different background *spa2Δ* (NY3022), *pea2Δ* (NY3023), *bud6Δ* (NY3024), and *bni1Δ* (NY3025), the same strategy was used to replace the entire coding sequences of each gene with the *S. pombe his5⁺* gene or the KanMX4 module in SEY6210, NY1211, or NY1210 yeast strain. The double mutants *pea2Δ ptc1Δ* (NY2964), *bni1Δ ptc1Δ* (NY2967), *msb3Δ ptc1Δ* (NY2972), *msb4Δ ptc1Δ* (NY2973), and *bud6Δ ptc1Δ* (NY2969), *spa2Δ ptc1Δ* (NY2975) were made from a cross between the corresponding single-deletion strain and NY2965 or NY2920. The double mutants *spa2Δ sec3Δ* (NY3026), *pea2Δ sec3Δ* (NY3027), and *bud6Δ sec3Δ* (NY3028) were made from a cross between the corresponding single-deletion strains and SFNY1153. *sph1Δ* (NY3030) is from the yeast genome-wide gene-deletion collection and was crossed to NY2959 to generate *sph1Δ ptc1Δ* (NY2960). NY2976 was generated by replacing the *MSB4* coding sequence in NY2970 with *TRP1* module by the PCR-mediated gene deletion method (Longtine *et al.*, 1998). NY3020 was generated by replacing the *SLT2* coding sequence in NY1210 with the *S. pombe his5⁺* module similarly. To visualize cER or mitochondria in living cells by microscopy, *Stul*-digested pRH475 integrating plasmid (Cronin *et al.*, 2000) or plasmid pYDY104 encoding a mitochondria-targeting sequence fused to the NH2 terminus of the red fluorescent protein (RFP; Du *et al.*, 2001) was transformed into each strain. To determine the subcellular localization of SlT2p or Mkk1p, plasmid pFD299 or pFD273 (generous gifts from Matthias Peter, Eidgenössische Technische Hochschule Zürich) was transformed into corresponding strains to detect GFP fluorescence.

Microscopy

For latrunculin A (Lat-A) treatment, wt or various mutant cells were grown in synthetic complete (SC) medium to log phase. Cells were then incubated with 200 μM Lat-A or control dimethyl sulfoxide for 10 min. Cells were washed, and images were acquired. For quantitation, after treatment, cells were immediately fixed in 4% formaldehyde at 25°C for 30 min and washed five times in phosphate-buffered saline (PBS) containing 1 mg/ml bovine serum albumin (BSA) and mounted in PBS-BSA for visualization.

The inheritance of ER and mitochondria was analyzed essentially as previously described (Du *et al.*, 2006). Cells were imaged on a Zeiss Axiophot 2 microscope (Carl Zeiss, Jena, Germany). Images were captured at 0.2-μm intervals along the z-axis using an ORCA-ER camera (Hamamatsu, Hamamatsu, Japan). All images shown were deconvolved with Openlab software (ImproVision, PerkinElmer, Waltham, MA).

Time-lapse microscopy of SFNY1684 (*ptc1Δ*) and SFNY1154 (*sec3Δ*) was performed on cells grown to early log phase in SC medium at 25°C. Cells were observed with an Axio Observer Z1 microscope (Zeiss) immediately after Lat-A treatment. Images were captured at 10-s intervals for 5 min using AxioVision 4.8 software (Zeiss).

Cell lysate extracts and immunoblotting

Yeast cells were grown to mid-exponential phase in yeast extract/peptone/dextrose or SC medium. For each strain an equal amount of cells was harvested, immediately frozen in liquid N₂, and then lysed by a rapid alkaline lysis procedure essentially as described in

Westfall *et al.* (2008). The activated SlT2p was monitored with a rabbit phospho-p44/p42 MAPK antibody (Cell Signaling Technology, Beverly, MA) that specifically detects dually phosphorylated SlT2p. The total SlT2p was detected with a mouse monoclonal Mpk1(E-9) antibody (sc-133189 from Santa Cruz Biotechnology, Santa Cruz, CA). Mouse phosphoglycerate kinase (Pgk1) monoclonal antibody was used to detect Pgk1p as a loading control. The density of gel blots was scanned using ImageJ software (National Institutes of Health, Bethesda, MD). To quantify the relative SlT2p activation, the density of the phospho-SlT2 band was divided by the density of Pgk1p, and the normalized phospho-SlT2p value of each strain was divided by the maximum value among the group.

ACKNOWLEDGMENTS

We thank Christina Howard for technical assistance. This study was supported by National Institutes of Health Grants GM073892 to P.N. and S.F.N. and GM 35370 to P.N. Salary support for S.F.N. was provided by the Howard Hughes Medical Institute.

REFERENCES

- Amberg DC, Zahner JE, Mulholland JW, Pringle JR, Botstein D (1997). Aip3p/Bud6p, a yeast actin-interacting protein that is involved in morphogenesis and the selection of bipolar budding sites. *Mol Biol Cell* 8, 729–753.
- Babour A, Bicknell AA, Tourtellotte J, Niwa M (2010). A surveillance pathway monitors the fitness of the endoplasmic reticulum to control its inheritance. *Cell* 142, 256–269.
- Cronin SR, Khoury A, Ferry DK, Hampton RY (2000). Regulation of HMG-CoA reductase degradation requires the P-type ATPase Cod1p/Spf1p. *J Cell Biol* 148, 915–924.
- Du Y, Ferro-Novick S, Novick P (2004). Dynamics and inheritance of the endoplasmic reticulum. *J Cell Sci* 117, 2871–2878.
- Du Y, Pypaert M, Novick P, Ferro-Novick S (2001). Aux1p/Swa2p is required for cortical endoplasmic reticulum inheritance in *Saccharomyces cerevisiae*. *Mol Biol Cell* 12, 2614–2628.
- Du Y, Walker L, Novick P, Ferro-Novick S (2006). Ptc1p regulates cortical ER inheritance via SlT2p. *EMBO J* 25, 4413–4422.
- Estrada P, Kim J, Coleman J, Walker L, Dunn B, Takizawa P, Novick P, Ferro-Novick S (2003). Myo4p and She3p are required for cortical ER inheritance in *Saccharomyces cerevisiae*. *J Cell Biol* 163, 1255–1266.
- Fehrenbacher KL, Davis D, Wu M, Boldogh I, Pon LA (2002). Endoplasmic reticulum dynamics, inheritance, and cytoskeletal interactions in budding yeast. *Mol Biol Cell* 13, 854–865.
- Jin Y, Taylor Eves P, Tang F, Weisman LS (2009). PTC1 is required for vacuole inheritance and promotes the association of the myosin-V vacuole-specific receptor complex. *Mol Biol Cell* 20, 1312–1323.
- Levin DE (2005). Cell wall integrity signaling in *Saccharomyces cerevisiae*. *Microbiol Mol Biol Rev* 69, 262–291.
- Li X, Du Y, Siegel S, Ferro-Novick S, Novick P (2010). Activation of the mitogen-activated protein kinase, SlT2p, at bud tips blocks a late stage of endoplasmic reticulum inheritance in *Saccharomyces cerevisiae*. *Mol Biol Cell* 21, 1772–1782.
- Loewen CJ, Young BP, Tavassoli S, Levine TP (2007). Inheritance of cortical ER in yeast is required for normal septin organization. *J Cell Biol* 179, 467–483.
- Longtine MS, McKenzie A 3rd, Demarini DJ, Shah NG, Wach A, Brachet A, Philippsen P, Pringle JR (1998). Additional modules for versatile and economical PCR-based gene deletion and modification in *Saccharomyces cerevisiae*. *Yeast* 14, 953–961.
- Manford AG, Stefan CJ, Yuan HL, Macgurn JA, Emr SD (2012). ER-to-plasma membrane tethering proteins regulate cell signaling and ER morphology. *Dev Cell* 23, 1129–1140.
- Moseley JB, Sagot I, Manning AL, Xu Y, Eck MJ, Pellman D, Goode BL (2004). A conserved mechanism for Bni1- and mDia1-induced actin assembly and dual regulation of Bni1 by Bud6 and profilin. *Mol Biol Cell* 15, 896–907.
- Reinke CA, Kozik P, Glick BS (2004). Golgi inheritance in small buds of *Saccharomyces cerevisiae* is linked to endoplasmic reticulum inheritance. *Proc Natl Acad Sci USA* 101, 18018–18023.
- Roeder AD, Hermann GJ, Keegan BR, Thatcher SA, Shaw JM (1998). Mitochondrial inheritance is delayed in *Saccharomyces cerevisiae* cells lacking the serine/threonine phosphatase PTC1. *Mol Biol Cell* 9, 917–930.

- Roemer T, Vallier L, Sheu YJ, Snyder M (1998). The Spa2-related protein, Sph1p, is important for polarized growth in yeast. *J Cell Sci* 111, 479–494.
- Sheu YJ, Santos B, Fortin N, Costigan C, Snyder M (1998). Spa2p interacts with cell polarity proteins and signaling components involved in yeast cell morphogenesis. *Mol Cell Biol* 18, 4053–4069.
- Tcheperegine SE, Gao XD, Bi E (2005). Regulation of cell polarity by interactions of Msb3 and Msb4 with Cdc42 and polarisome components. *Mol Cell Biol* 25, 8567–8580.
- van Drogen F, Peter M (2002). Spa2p functions as a scaffold-like protein to recruit the Mpk1p MAP kinase module to sites of polarized growth. *Curr Biol* 12, 1698–1703.
- Voeltz GK, Rolls MM, Rapoport TA (2002). Structural organization of the endoplasmic reticulum. *EMBO Rep* 3, 944–950.
- Westfall PJ, Patterson JC, Chen RE, Thorner J (2008). Stress resistance and signal fidelity independent of nuclear MAPK function. *Proc Natl Acad Sci USA* 105, 12212–12217.
- Wiederkehr A, Du Y, Pypaert M, Ferro-Novick S, Novick P (2003). Sec3p is needed for the spatial regulation of secretion and for the inheritance of the cortical endoplasmic reticulum. *Mol Biol Cell* 14, 4770–4782.
- Zarzov P, Mazzoni C, Mann C (1996). The SLT2(MPK1) MAP kinase is activated during periods of polarized cell growth in yeast. *EMBO J* 15, 83–91.